In Situ Characterization of Functional Purple Membrane Monolayers at the Air−Water Interface

Mario Méthot,[†] Philippe Desmeules,[†] David Vaknin,[‡] François Boucher,[§] and Christian Salesse*,[†]

Unité de recherche en ophthalmologie, Centre de recherche du CHUQ, Université Laval, Québec, Québec, Canada, G1V 4G2, Ames Laboratory and Department of Physics, Iowa State University, Ames, Iowa 50011, and GREIB, Département de Chimie-Biologie, Université du Québec à Trois-Rivières, Trois-Rivières, Québec, Canada, G9A 5H7

Received August 29, 2003. In Final Form: November 19, 2003

The purple membrane (PM) of *Halobacterium salinarum* contains a single type of protein, bacteriorhodopsin (bR), which is a member of the seven α-helices transmembrane protein family. This protein is a photoactive proton pump, translocating one proton from the cytoplasmic to the extracellular side of the PM per photon absorbed. bR is found in trimers in PM, where they are assembled in a two-dimensional hexagonal lattice. We show herein that stable and functional films can be built in monolayers at the air−water interface by spreading aqueous suspensions of purified and native PM patches. In situ spectroscopic measurements at the air−water interface indicate that bR remains photoactive in this environment. Physical parameters of these PM films, such as protein molecular area, irreversible in-plane aggregation, *z*-axis orientation, film thickness, and surface roughness, were determined from surface pressure and surface potential−area isotherms, fluorescence spectroscopy, and X-ray reflectivity at the air−water interface. We find that PM do form organized monolayers of membranes, with an optimal packing density at a surface pressure of approximately 20 mN/m, although no preferential vectorial alignment, with respect to the plane normal to the membrane, can be detected from fluorescence quenching experiments.

Introduction

Since the mid-1980s, the purple membrane (PM) of *Halobacteria* has often been proposed as a basis for a wide spectrum of biological and technological studies and applications ranging from high-speed optical random access memory[1,2] to artificial photoreceptors.[3] This interest is mostly due to the properties of its sole protein, bacteriorhodopsin (bR), which represents 75% of PM by weight.[4] Important virtues of this transmembrane protein are its stability within a wide range of pH and temperature, its ability to pump protons upon light absorption, and the possibility of getting very thin (one layer thick) films of photoactive bR.[5,6] Since in most cases, proposals for bR-based electrooptic devices include the transfer of purple membrane monolayers from water surface to a solid semiconductor support, precise characterization of PM monolayers is of crucial importance.

The goal of the present study was to investigate and characterize, in situ, the functional and structural properties of native PM films in monolayers at the air−water interface. Previous studies of this system have focused on PM mixed with organic solvents such as *N*,*N*-dimethylformamide and hexane[7] or with exogeneous lipids such as soya-PC[8,9] to form monolayers at the air−water interface. The motivation of forming PM monolayers under these conditions was to maintain the same protein structure as "they exhibit in the spreading solvent"[7] and also to prevent PM aggregation that could lead to protein loss into the subphase.[10] We believe, on the contrary, that in order to get the most effective PM films in terms of bR photoactivity, one should spread PM monolayers under conditions as close as possible to the physiological conditions. It is well-known, for example, that treatment of PM with small concentrations of organic solvents such as hexane can lead to impressive changes in the structure and properties of bR.[11,12] On the other hand, intact PM membranes were recently reported to retain their native crystalline character at the air−water interface.[13]

The effects of solvents[14] or lipids[15] cannot be neglected in order to set proper conditions for the development of highly effective PM films. We thus performed measurements of surface pressure and surface potential−area isotherms, as well as compression−decompression−recompression (CDR) cycles, together with absorption and fluorescence spectroscopies along with X-ray reflectivity measurements, of pure PM films at the air−water interface. This set of methods shows that PM forms a membrane

* To whom correspondence should be addressed: e-mail christian.salesse@crchul.ulaval.ca.

† Unité de recherche en ophthalmologie, CHUL.

‡ Iowa State University.

§ Université du Québec à Trois-Rivières.

(1) Birge, R. R. *Annu. Rev. Phys. Chem* **1990**, *41*, 683−733.
(2) Birge, R. R. *Sci. Am.* **1995**, *272*, 90−95.
(3) Min, J.; Choi, H. G.; Oh, B. K.; Lee, W. H.; Pack, S. H.; Choi, J. W. *Biosens. Bioelectron.* **2001**, *16*, 917−923.
(4) Oesterhelt, D.; Stoeckenius, W. *Nat. New Biol.* **1971**, *233* (39), 149−52.
(5) Hampp, N. *Nat. New Biol.* **1993**, *366*, 12.
(6) Shen, Y.; Safinya, C. R.; Liang, K. S.; Ruppert, A. F.; Rothschild, K. J. *Nature* **1993**, *366*, 48−50.
(7) Hwang, S. B.; Korenbrot, J. I.; Stoeckenius, W. *J. Membr. Biol.* **1977**, *36*, 115.
(8) Ikonen, M.; Peltonen, J.; Vuorimaa, E.; Lemmetyinen, H. *Thin Solid Films* **1992**, *213*, 277.
(9) Flanagan, M. T. *Thin Solid Films* **1983**, *99*, 133−138.
(10) Schildkraut, J.; Lewis, A. *Thin Solid Films* **1985**, *134*, 13−26.
(11) Messaoudi, S.; Lee, K. H.; Beaulieu, D.; Baribeau, J.; Boucher, F. *Biochim. Biophys. Acta* **1992**, *1140*, 45.
(12) Messaoudi, S.; Daigle, I.; Boucher, F. *J. Mol. Struct.* **1993**, *297*, 19−27.
(13) Verclas, S. A. W.; Howes, P. B.; Kjaer, K.; Wurlitzer, A.; Weygang, M.; Buldt, G.; Dencher, N. A.; Losche, M. *J. Mol. Biol.* **1999**, *287*, 837−843.
(14) Eisenbach, M.; Caplan, S. R. *Biochim. Biophys. Acta* **1979**, *554* (2), 281−92.
(15) Hendler, R. W.; Dracheva, S. *Biochemistry (Moscow)* **2001**, *66* (11), 1311−4.

10.1021/la0356147 CCC: $27.50
Published on Web 12/30/2003

monolayer at the air−water interface, with an optimal packing density at a surface pressure of approximately 20 mN/m. Moreover, we also demonstrate that bR remains photoactive in this environment. However, PM do not preferentially orient with respect to the *z*-axis, as their sidedness appears completely random.

Experimental Details

Chemicals used throughout the work were from Baxter (Mississauga, Canada) and of the finest available grade. Sodium chloride used at high concentrations to prepare subphase buffers was purified by multiple extractions from chloroform.[16] Highly concentrated potassium iodide solutions used in the fluorescence quenching experiments also contained 2 mM $Na_2S_2O_3 \cdot 5H_2O$ to prevent iodide oxidation.

PM were isolated and purified from the S-9 strain of *Halobacterium salinarum* according to the method of Kates et al.[17] to yield membrane patches of 0.5−1.0 μm in size. They were then suspended in a conservation medium containing 4.3 M NaCl, 27 mM KCl, and 81 mM $MgSO_4 \cdot 7H_2O$ and stored at 4 °C until needed. Prior to use, an aliquot of this suspension is washed three times by centrifugation at 17500*g* and resuspended in deionized water (resistivity > 18 MΩ cm) at a bR concentration of 10^{-5} M, as determined by absorption spectroscopy (using $\epsilon =$ 58 000 M^{-1} cm^{-1}). Fluorescent labeled PM were prepared by binding fluorescein isothiocyanate to the only water-exposed lysine of bR (K_{129}) lying on the extracellular side of the membrane as described by Heberle and Dencher.[18]

Surface−pressure (π) and surface potential−area ($\Delta V-A$) isotherms were measured with fully automated Langmuir troughs equipped with a Wilhelmy plate, and an ^{241}Am electrode, as previously described.[19] Absorption and fluorescence spectroscopic measurements of monolayers were obtained with an interface spectrophotometer of our own, whose characteristics have also been published elsewhere.[19] For the fluorescence quenching experiments, the monolayer trough was fitted with a restriction mask made from ceramic. It consists essentially of an open-end vertical cylindrical well ($\phi = 7.5$ cm), deposited on the bottom of the trough, whose top border exceeds the water surface by ~1 mm. A 3 cm door on the side of the cylindrical well allowed the monolayer under compression to enter onto the aqueous surface of the well. Once the desired surface pressure was obtained and stabilized, the 3 cm side opening of the well was closed with a tight sliding door, thus considerably restricting the area under study. Fluorescence spectra taken before and upon closing of the well (results not shown) always showed no significant difference in shape or intensity, thus ensuring that closing of the well did not significantly perturb the PM monolayer. This procedure allowed us to use much smaller quencher volumes as the quencher solution was added only to the cylinder volume instead of the whole trough volume. Furthermore, any quencher injection in the restricted subphase was compensated by withdrawal of an equal volume of subphase buffer in order to keep the restricted surface at the very same water level, a necessary condition to achieve accurate surface fluorescence measurements. Quantitative assessment of bR (and hence, PM) orientation was done by use of the modified Stern−Volmer equation[20] for the special case of two distinct fluorophore populations, F_a and F_b, standing respectively for the accessible and inaccessible fluoresceins. A plot of $F_0/\Delta F$ vs 1/[Q] yields the value of f_a when $F_0/\Delta F$ is extrapolated to infinite quencher concentration.

Monolayer X-ray reflectivity measurements of spread films were carried out on the liquid surface X-ray reflectometer at Ames National Laboratory. The apparatus is similar to that described by Als-Nielsen and Pershan,[21] with the additional ability to rotate the θ and 2θ arm of the monochromator to obtain additional degrees of freedom that allow second-order corrections of the two axes. These corrections ensure operation with a constant wavelength ($\lambda = 1.5404$ Å) at all scattering angles. Calculations were performed by standard procedures with specular reflectivity, as a function of the momentum-transfer ($Q_Z = 4\pi/\lambda$) defined as

$$\frac{I_r}{I_0} = R(Q_Z)$$

where I_r and I_0 stand for the reflected and incident beam intensity, respectively.

To account for capillary waves and surface imperfections, Gaussian-smeared interfaces were assumed to have the form

$$\exp\left\{\frac{-0.5(z - z_i)^2}{\sigma^2}\right\}$$

where σ is the surface roughness. Accordingly, the reflectivity was corrected by a Debye−Waller-like factor such as

$$R(Q_Z) = R_0(Q_Z)e^{-(Q_Z\sigma)^2}$$

Prior to film spreading, a complete compression curve was recorded for the buffer alone, and no surface pressure could be detected, ensuring that the surface was free from tensioactive contaminants. Given the high protein content of PM and following the suggestions by Gaines[22] and Pattus et al.,[23] we have built monolayers by dropwise spreading of an aqueous suspension of purified PM from a microsyringe onto the Langmuir trough filled with 43 mM carbonate buffer (pH 9), containing 0.1 M NaCl (unless otherwise stated). This buffer was used for all experiments presented herein. Building the PM monolayer was achieved very slowly by spreading very small drops at different spots across the surface; covering a 200 cm^2 surface could take more than 1 h, after which the monolayer was allowed to equilibrate for one additional hour. Then, compression could be started at a constant speed of 68 $Å^2$/(bR molecule·min). Films constructed according to this procedure were very stable; typically, once compressed between 5 and 40 mN/m and allowed to stand, the surface pressure lowered by less than 1.5 mN/m during the first 15 min and then remained stable for hours. It is noteworthy to mention that isotherms performed on 4 M NaCl mandated the use of a custom-built chamber that covered the whole trough, where humidity levels could be maintained at >80% by use of a small cold-mist humidifier, thus minimizing evaporation and salt crystallization on the filter paper of the Wilhelmy plate.

CDR cycles using PM films were performed in a similar way as the previously described $\pi-A$ isotherms, except that once the desired maximal surface pressure was attained, films were immediately decompressed until $\pi = 0$ mN/m (unless otherwise stated). Films were then left to relax for 5 min before being recompressed again to the same maximal surface pressure. CDR isotherms were thus recorded for maximal surface pressures of 10, 20, 30, 40, and 46 (collapse pressure) mN/m. Surface potential−area isotherms were simultaneously recorded along with those surface pressure CDR isotherms.

Results

As the ultimate goal of building one-molecule-thick films of bR to assemble bioelectronic devices mandates the use of a functional protein, it was thus essential to make sure that bR was not denatured and was still photoactive at the air−water interface. To ascertain bR functionality in monolayers, absorption spectroscopy measurements were performed in situ, at the air−water interface, on dark-

(16) Gallant, J.; Desbat, B.; Vaknin, D.; Salesse, C. *Biophys. J.* **1998**, *75*, 2888−2899.
(17) Kates, M.; Kushwaha, S. C.; Sprott, G. D. *Methods Enzymol.* **1982**, *88*, 98.
(18) Heberle, J.; Dencher, N. A. *Proc. Natl. Acad. Sci. U.S.A.* **1992**, *89*, 5996−6000.
(19) Gallant, J.; Lavoie, H.; Tessier, A.; Munger, G.; Leblanc, R. M.; Salesse, C. *Langmuir* **1998**, *14*, 3954−3963.
(20) Lakowicz, J. R. *Principles of Fluorescence Spectroscopy*, 2nd ed.; Kluwer Academic/Plenum Publishers: New York, 1999.
(21) Als-Nielsen, J.; Pershan, P. S. *Nucl. Inst. Methods* **1983**, *208*, 545.
(22) Gaines, J. G. L. *Insoluble monolayers at liquid/gas interfaces*; Interscience Ed.: New York, 1966.
(23) Pattus, F.; Rothen, C.; Streit, M.; Zahler, P. *Biochim. Biophys. Acta* **1981**, *647* (1), 29−39.

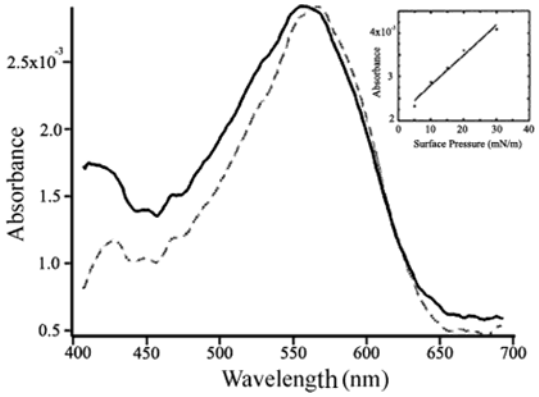

Figure 1. : Absorption spectra of a PM film at the air−water interface (π = 5 mN/m): dark- (solid line) and light-adapted (dashed line) states of PM films. Inset: Peak absorbance is plotted against surface pressure from 5 to 30 mN/m for dark-adapted PM films.

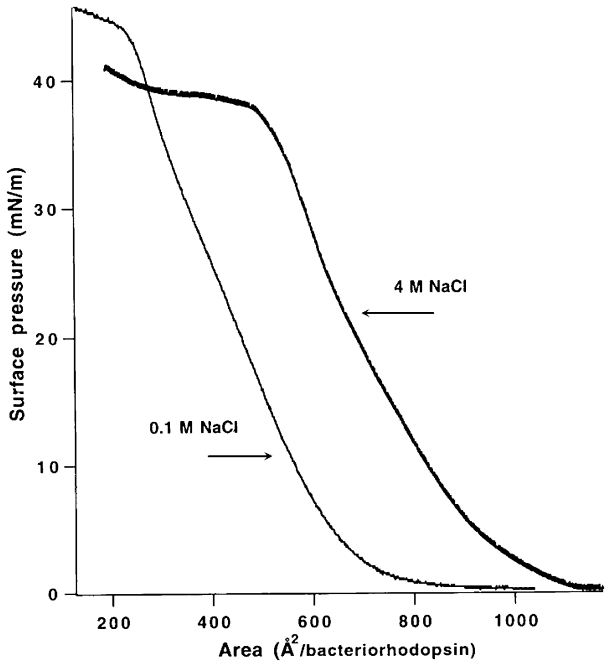

Figure 2. Surface pressure−area (π−A) isotherms of purple membrane films at the air−water interface on a subphase containing 100 mM or 4 M NaCl.

adapted and light-adapted PM. Working under dim green light, films were compressed to the desired surface pressure. After stabilization, light was switched off and the film was maintained under complete darkness for 30 min to achieve dark adaptation. Spectra were then taken and the film was thereafter irradiated with a heat-filtered 150 W white light for 30 min in order to adapt bR to light. Spectra were taken immediately after the irradiation was stopped.

As shown in Figure 1, light activation caused a 10 nm red shift of the spectrum of PM, moving the absorption maximum from 560 to 570 nm. This shift is very well characterized for PM suspensions[4] and corresponds to a 13-cis to all-trans photoisomerization of the protein's retinal chromophore. It is a sensitive indication regarding the photochemical functionality of bR. In addition, as shown in the inset, the absorbance vs pressure plot in the 5−30 mN/m range is linear. In addition, the surface pressure vs molecular area (see isotherms in Figure 2) is almost linear within the same surface pressure range (5−30 mN/m). The fact that the absorbance of PM also follows a linear dependence is an indication of the stability and homogeneity of the film.

Surface Pressure Isotherms. Building molecular monolayers from native purple membrane patches is quite a tricky business since it is constituted of a 2D crystal of bacteriorhodopsin, and instead of self-organizing as a uniform monolayer onto the water surface, they tend to sink into the aqueous subphase. In fact, like others who have tried before, we were unable to measure any surface pressure signal after spreading PM on pure water. Nevertheless, alternate procedures are available, involving spreading of various mixtures composed of phosphatidylcholine/purple membrane/hexane and, sometimes, dimethylformamide.[8−10,24−30] However, all of these methods suffer from the same flaws: at best, they lower by up to 300% the surface density of bacteriorhodopsin due to the presence of exogeneous lipids; at worst, they induce irreversible structural modifications.[11,12] We also have evidence from X-ray diffraction and atomic force microscopy that exposure of PM to minute amounts of organic solvents destroys the crystalline character of the PM patches (to be published elsewhere).

The isotherms obtained for intact purple membranes spread on 0.1 and 4 M NaCl are shown in Figure 2. On a 0.1 M NaCl buffered subphase, the lift-off is at ∼850 Å²/bR. Most likely due to equilibration between surface and bulk subphase PM, the lift-off area is poorly reproduced from one measurement to another. However, reproducibility of the π values for curve inflections and collapse is better than 2%. Upon compression, purple membrane monolayers always show a kink near 20 mN/m, approximately midway between the lift-off and the collapse pressure (46 mN/m).

On the 4 M NaCl buffered subphase, the π−A isotherm shows essentially the same features as on the low-salt buffer, except for the higher area/bR values, which reach ∼1100 Å²/bR at lift-off, and for its collapse pressure, which is reduced by 20% due to the lower surface tension of the high-salt buffer. However the reproducibility of the lift-off area is better than on the low-salt buffer, a typical variation of ±10% was observed from one PM film to the next. Reduced sinking of membranes into the subphase is the most likely explanation for this increase in molecular area and better reproducibility. In fact, if all deposited membranes remained on the water surface, we should expect a molecular area value of at least 1200 Å²/bR, on the basis of the area initially determined by electron microscopy[31] and confirmed more recently at high resolution by X-ray diffraction.[32] Given the proverbial stability of PM, it is unlikely that the discrepancy between the measured and the effective cross section of bR could be due to denaturation. In fact, in contrast to our experiments where a smaller area is observed, denaturation results in a larger surface area occupied by the denatured protein.[19] Anyhow, denaturation does not occur under our experi-

(24) Hwang, S. B.; Korenbrot, J. I.; Stoeckenius, W. *J. Membr. Biol.* **1977**, *36* (2−3), 115−35.
(25) Ikonen, M.; Sharonov, A.; Tkachenko, N.; Lemmetyinen, H. *Adv. Mater. Opt. Electron.* **1993**, *2*, 115−122.
(26) Hu, K. S.; Wang, A. J.; Tan, M. Q.; Li, J. T.; Jiang, L. *Chin. Sci. Bull.* **1992**, *37*, 231−234.
(27) Lemmetyinen, H.; Ikonen, M.; Sharonov, A.; Tkachenko, N. *SPIE* **1992**, *1921*, 209−220.
(28) Du, W.; Liu, S. *Thin Solid Films* **1993**, *229*, 122−127.
(29) Miyasaka, T.; Koyama, K.; Itoh, I. *Science* **1992**, *255*, 342−344.
(30) Choi, H. G.; Jung, W. C.; Min, J.; Lee, W. H.; Choi, J. W. *Biosens. Bioelectron.* **2001**, *16* (9−12), 925−35.
(31) Henderson, R.; Unwin, P. N. T. *Nat. New Biol.* **1975**, *257*, 28−32.
(32) Pebay-Peyroula, E.; Rummel, G.; Rosenbusch, J. P.; Landau, E. M. *Science* **1997**, *277* (5332), 1676−81.

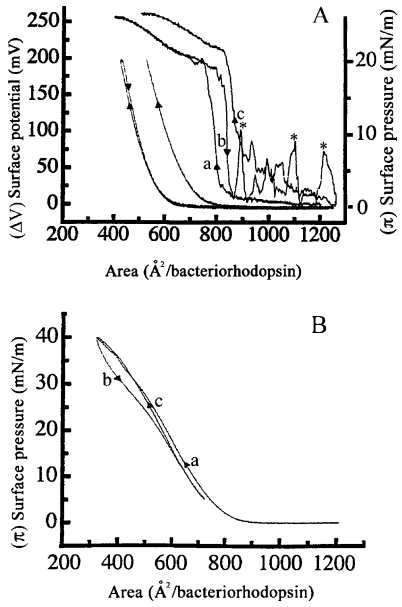

Figure 3. Compression (curves a), decompression (curves b), and recompression (curves c) isotherms of PM films measured on 100 mM NaCl subphase. Compression and decompression were done at a speed of 68 Å²/(bR molecule•min). (A) Surface pressure−area and simultaneously recorded surface potential isotherms area (curves a−c). Asterisks point to some of the spontaneous jumps in surface potential. Maximal surface pressure during the compression step = 20 mN/m. (B) Surface pressure−area isotherms where the maximal surface pressure attained during the compression step = 40 mN/m. Decompression is stopped at a minimum surface pressure of 5 mN/m and held at that pressure for 5 min before recompression.

mental conditions as demonstrated by polarization-modulated infrared reflection absorption spectroscopy (PM-IRRAS)[33,34] and as also attested by the previously shown results obtained by absorption spectroscopy (Figure 1). On the other hand, X-ray reflectivity results shown herein clearly demonstrate that multilayer formation does not occur at moderate surface pressures. Thus, the fact that on a high-salt subphase the apparent cross-section value at lift-off reaches approximately 90% of the value obtained from the electron microscopy data allows us to conclude that the smaller molecular areas that we observed on the 0.1 M salt buffer simply resulted from more important PM loss into the subphase. This is further supported by the measurement of the CDR cycles (see below).

PM Aggregation upon Compression. Schildkraut and Lewis[10] have previously hypothesized that the lateral pressure applied to a film of PM at the air−water interface could promote a reversible aggregation of the PM fragments if the film is compressed to a maximal surface pressure of 20 mN/m. However, films that underwent compression to surface pressures above 35 mN/m showed an irreversible behavior (based on their CDR cycles) that they attributed to PM loss into the subphase. Our experimental conditions being substantially different from theirs (different buffer composition, and use of hexane in the spreading solution in Schildkraut and Lewis' experiments), we proceeded with our own set of CDR experiments.

As can be seen in Figure 3A for maximal surface pressures of 20 mN/m during the compression step, no significant hysteresis could be detected between the compression and decompression curves, the two curves being almost overlaid. However, the recompression curve is strongly shifted toward larger molecular areas (∼25% increase in molecular area at lift-off). This latter phenomenon was systematically observed for all maximal surface pressures attained during the compression step when the film was decompressed to maximum molecular area and left to relax for 5 min prior to recompression.

The simultaneously recorded surface potential−area isotherms (Figure 3A) display a similar behavior, the compression (curve a) and decompression (curve b) curves being overlaid for $\pi > 0$ mN/m, while the recompression curve (curve c) is also shifted toward larger molecular areas. It is noteworthy that the maximum value of surface potential is already reached at a surface pressure of 20 mN/m and is the same whether in the compression, decompression, or recompression step. However, the signal amplitude varies considerably from one experiment to the other. Of special interest is the presence of significant spontaneous jumps in surface potential at $\pi = 0$ mN/m, observed in the decompression and recompression curves (see asterisks on Figure 3A) but completely absent from the compression curve. Those spontaneous jumps start to appear when the maximal surface pressure attained during the compression step is ≥20 mN/m and are attributed to the formation of in-plane aggregates of PM patches that pass randomly under the ^{241}Am electrode at $\pi = 0$ mN/m.

The scenario is, however, different when films were compressed to 30 mN/m or beyond. Figure 3B presents a typical CDR cycle where a PM film was compressed to a maximal surface pressure of 40 mN/m and then decompressed to a minimum surface pressure of 5 mN/m (instead of 0 mN/m) and held for 5 min at this surface pressure before recompression. Those results clearly show that, on one hand, a pronounced hysteresis between the compression and decompression curves becomes apparent and thus demonstrates that some irreversible phenomenon is taking place in the PM films compressed to 30 mN/m or more (results not shown). On the other hand, the recompression curve is no longer shifted toward larger molecular areas. At this point, we hypothesize that when films are fully decompressed (to $\pi = 0$ mN/m) and maintained in this expanded state for a few minutes prior to recompression, PM patches that were lost into the subphase during film spreading could be reinserted in the film and thus lead to a shift toward larger molecular areas on the surface pressure isotherm. However, a minimum surface pressure of 5 mN/m maintained during the decompression step would be sufficient to prevent PM reinsertion in the film and would thus explain the fact that no shift toward larger molecular areas is observed when films are not fully expanded during decompression.

Figure 4 shows the calculated isothermal inverse compressibility $[1/K_S = -A(\delta\pi/\delta A)_T]$ of the $\pi-A$ curve and the measured surface potential isotherm obtained on the subphase containing 0.1 M NaCl (the surface pressure isotherm is also shown for comparison). The coincidence is striking as, in both cases, a maximum is obtained at ∼500 Å²/bR, which corresponds to a surface pressure of approximately 20 mN/m on the isotherm. It seems obvious that both the mechanical (surface pressure) and electrical (surface potential) behavior of the PM film at this surface pressure point to a common underlying phenomenon. We thus put forward the hypothesis that a surface pressure of approximately 20 mN/m represents the pressure at which the monolayer reaches its optimally packed organization. Beyond that point, some irreversible phenomena

(33) Blaudez, D.; Boucher, F.; Buffeteau, T.; Desbat, B.; Grandbois, M.; Salesse, C. *Appl. Spectrosc.* **1999**, *53*, 1299−1304.
(34) Lavoie, H.; Gallant, J.; Grandbois, M.; Blaudez, D.; Desbat, B.; Boucher, F.; Salesse, C. *Mater. Sci. Eng.* **1999**, *10*, 147−154.

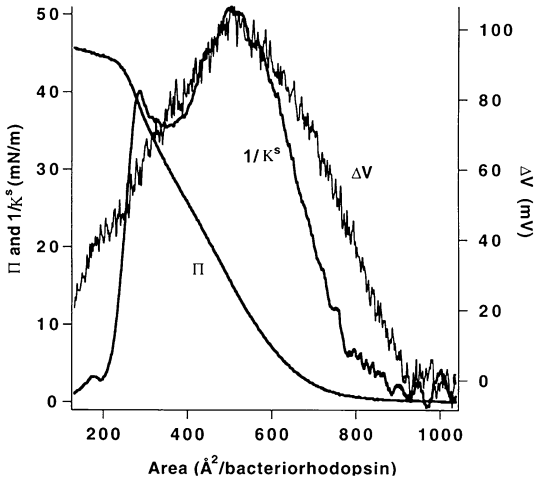

Figure 4. Surface pressure isotherm (Π), inverse compressibility ($1/K_S$), and surface potential (ΔV) for a purple membrane film on a 100 mM NaCl subphase.

lead to the appearance of a hysteresis in the CDR isotherms, while the decrease in both K_S and ΔV could find its origin in monolayer sinking, in stacking of membranes, and/or in reorientation of the bR contained in the purple membrane patches. However, this latter possibility has been ruled out by previous attenuated total reflection (ATR) infrared spectroscopic measurements,[35] as well as by in situ PM-IRRAS at the air−water interface,[34] since both approaches led to the conclusion that such a bR reorientation was not occurring within this surface pressure range.

Monolayer Thickness and Homogeneity. X-ray reflectivity measurements at the air−water interface allow the in situ characterization of the PM film from which its *z* dimension (thickness) and its homogeneity (surface roughness) can be extracted. Figure 5 presents a typical reflectivity curve of a PM film at 26 mN/m, normalized to the Fresnel reflectivity expected for an interface where the electron density, $\rho(z)$, changes abruptly from air ($\rho = 0$) to water ($\rho = 0.334$ e/Å^3). We define the "homogeneous thickness" (d_H) as the sum of the lengths of all boxes in the absence of any interfacial roughness (i.e, $\sigma = 0$ in the box model). In this case, the film consists of a single slab of homogeneous electron density (see refs 36 and 37), which graphically translates into a box model as shown in the inset of Figure 5. The "total thickness" (d_T) is our definition for the thickness of the film including the contribution of interfacial roughness to the "homogeneous thickness". We systematically take the total thickness to be $d_T = d_H + 4\sigma$ (σ is the effective roughness extracted from the reflectivity; the constant 4 arbitrarily represents the point where the interfacial density falls off to about 10%). The effective surface roughness, σ, has contributions from capillary waves (σ_C) and from the intrinsic (static) morphology of the film (σ_I), given by $\sigma = (\sigma_C^2 + \sigma_I^2)^{1/2}$. From our experiments and others we know that the surface roughness due to capillary waves is much smaller ($\sigma_C \sim 2.4$ Å) than that measured for the protein film at the interface (i.e., $\sigma_I > \sigma_C$, and therefore $\sigma = (\sigma_C^2 + \sigma_I^2)^{1/2} \sim \sigma_I$), so it becomes reasonable to assume that the measured roughness represents a major contribution from the intrinsic roughness of the film, altough some minor contribution from capillary waves cannot be totally ruled out. In calculating the reflectivities, it was assumed that the interface consists of a single slab[36,37] of homogeneous

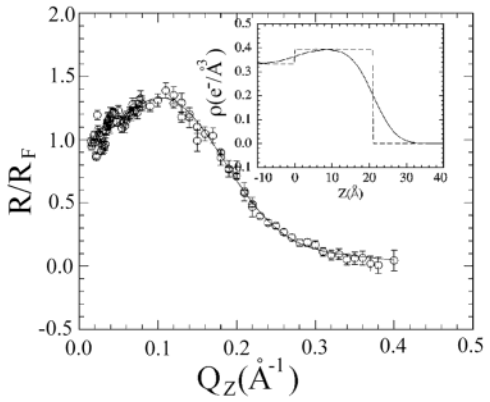

Figure 5. X-ray normalized reflectivity of a PM film at the air−water interface (in this case, $\pi = 26$ mN/m). The solid line is calculated from the electron density profile shown in the inset. The dashed line in the inset illustrates the ideally sharp interfaces that are Gaussian-smeared due to surface roughness to yield the solid line. The total film thickness thus corresponds to the region where the electron density grows higher than water electron density (0.334 e/Å^3), goes to a maximum, and falls back to the air electron density (∼0 e/Å^3). The homogeneous thickness is defined as the region corresponding to the middle half Gaussian distribution (dashed lines), i.e., to an ideal region of homogeneous electron density along the *z* axis, having sharp interfaces and containing all the electrons attributed to the monolayer in this direction. The surface roughness refers to the extension of Gaussian-smearing from this ideally sharp *slab* of homogeneous electron density and can be visualized as a film surface topography indicator.

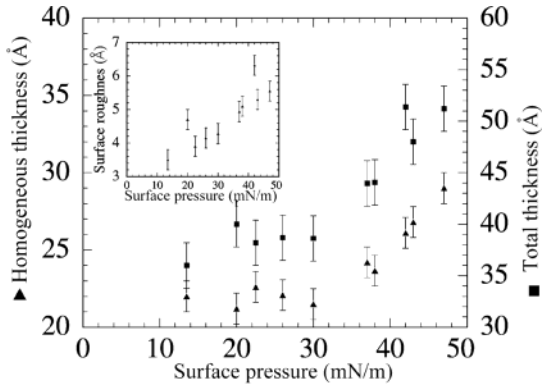

Figure 6. Total film thickness (■), homogeneous thickness (▲), and surface roughness (inset, ▲), plotted against lateral pressure for PM films at the air−water interface.

electron density. Reflectivity curves were taken on PM films within a 10−47 mN/m surface pressure range, a new film being prepared for each measurement. Results are summarized in Figure 6 and expressed in terms of total and homogeneous thickness as a function of the lateral pressure.

The total thickness of the film remains almost unchanged at 38 Å (±2 Å) for surface pressures below 35 mN/m (just before the collapse, which occurs at ∼43 mN/m), while a homogeneous thickness value of 22 Å is found at the same π values. This measured total thickness is in excellent agreement with the experimental[38] and calculated[39] distance between lipid polar headgroups

(35) Méthot, M.; Subirade, M.; Pézolet, M.; Boucher, F.; Salesse, C. *Thin Solid Films* **1996**, *627*, 284−285.

(36) Als-Nielsen, J.; Kjaer, K. *Proc. NATO ASI Ser. B 211*; Plenum Press: New York, 1989.

(37) Als-Nielsen, J.; Jacquemain, D.; Kjaer, D.; Lahav, M.; Leveiller, F.; Leiserovitz, L. *Phys. Rep.* **1994**, *246*, 251−313.

(38) Lewis, B. A.; Engelman, D. M. *J. Mol. Biol.* **1983**, *166* (2), 203−10.

(39) Edholm, O.; Berger, O.; Jahnig, F. *J. Mol. Biol.* **1995**, *250* (1), 94−111.

across the purple membrane, which is estimated at 40 Å, and also corresponds to the value of 40 Å for the length of the α-helices, as originally measured by Henderson and Unwin[31] by electron microscopy. Within the same surface pressure range, the surface roughness (shown in the inset) slightly increases from 3.5 to 4 Å. Although this range of values is typical for lipid monolayers, it also agrees with other data since a membrane roughness of ≥4 Å can directly be measured for purple membranes by atomic force microscopy.[40]

From 37 mN/m and over, there is a sharp increase in film thickness and surface roughness. While the surface roughness increase can be partly accounted for by the lowering of the surface tension,[36] and also by the intrinsic roughness of the film constituents,[16] the increasing thickness values from 38 to 51 Å strongly suggest that at such high surface pressure values, near that of the collapse, some membrane stacking is taking place. Measurements were also done at pressures as low as 1 mN/m (results not shown) but coarse surface roughness prevented any reasonable fitting of the reflectivity curves, most probably due to a poor surface coverage by PM patches ("holes" in the film). The most likely sketch that we can get from these data is as follows: At very low surface pressure (∼1 mN/m), the water surface is poorly covered with PM patches and high roughness values are observed. In the 10−30 mN/m pressure range, a PM monolayer is formed. Within this surface pressure range, the membrane roughness is in full agreement with that observed by atomic force microscopy and can be attributed to the native uneven alignment of the bR helices, interhelical loops, and lipid bilayer, which fill spaces between individual and trimeric bacteriorhodopsin molecules. Above 35 mN/m, the thickness and roughness increase rules out the previously mentioned possibility of PM sinking discussed in the CDR results section, as this event would not lead to an increase in film thickness. In addition, this increase is too large to be compatible with molecular reorganization of structural elements such as loops or helix and must have its origin on a much larger scale due to the progressive build-up of a second PM layer. As a matter of fact, FTIR-ATR spectroscopy of transferred purple membrane films,[35] as well as PM-IRRAS measurements at the air−water interface,[34] have shown that the orientation of the bR helices remains unchanged within the range of surface pressures studied herein.

Membrane Orientation at the Air−Water Interface. Between 10 and 35 mN/m, a PM film can be viewed as a uniform membrane monolayer. In view of their strong permanent dipole (4×10^{-24} C·m) due mostly to asymmetric lipid and surface charge distribution,[41] it could be conceived that PM would spontaneously orient their extracellular side toward the water surface. We have thus investigated that possibility by quenching the fluorescence of PM patches whose extracellular side was tagged with fluorescein using aqueous KI injected into the subphase. The modified Stern−Volmer plot for quenching experiments done with PM films at the air−water interface is shown in Figure 7. While iodine is able to quench 100% of the fluorescence of aqueous membrane suspensions (inset of Figure 7), quencher concentrations up to 2.5 M only quenched 50% of the fluorescence when membranes are spread in monolayer. This result indicates that half of the fluorophores are accessible to aqueous KI added into the subphase and that the orientation of the membranes is random. This is a direct demonstration that PM do not show a preferred orientation when spread at the air−water interface, despite their strong electrostatic asymmetry.

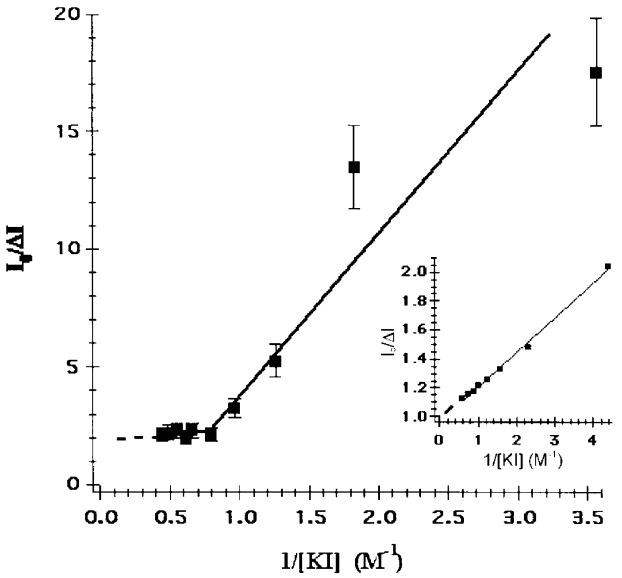

Figure 7. Stern−Volmer plot for the quenching of fluorescein-labeled PM at air−water interface upon KI addition in the subphase (see Materials and Methods for details of the procedure).

Discussion

In our experiments, purified PM patches, where bacteriorhodopsin is solvated only by its native lipids, do form functional, homogeneous, and stable monolayers between 10 and 35 mN/m. Evidence for this comes from the observed stability of the π values for spread monolayers, as well as from in situ absorption spectroscopy, surface potential, and X-ray reflectivity measurements. However, most likely due to heavy hydration of membrane surfaces, these PM are easy to suspend in water and quantitative surface spreading can hardly be achieved. As a matter of fact, the amount of membranes lost into the aqueous subphase can be minimized under high salt concentration conditions. We have also demonstrated that partial PM reinsertion in the film is possible between compression and recompression cycles inasmuch as the film is decompressed to $\pi = 0$ mN/m and maintained in this expanded state for a few minutes before recompression.

Fluorescence quenching of labeled membrane samples show no preferential orientation with respect to the axis normal to the membrane plane, despite their asymmetric charge distribution. This might find its origin in the fact that, in a dielectric medium such as buffered water, both membrane surfaces become electrostatically equivalent when viewed from a few Debye lengths distance. Thus, internal electrostatic asymmetry of bR cannot dictate any orientation of PM upon spreading of these patches. Interestingly, Nicolini et al.[42] have developed an electric field-assisted method of PM monolayer formation in unbuffered subphase that according to them results in highly oriented bR film formation. Their assumption is based on the observation of larger "light-on" currents compared to bR films produced without electrical field. However, it is well-known that locally induced pH changes generated under continuous illumination of immobilized

(40) Muller, D. J.; Heymann, J. B.; Oesterhelt, F.; Moller, C.; Gaub, H.; Buldt, G.; Engel, A. *Biochim Biophys Acta* **2000**, *1460* (1), 27−38.
(41) Taneva, S. G.; Petkanchin, I. B. *Photobiology*; Plenum Press: New York, 1992.
(42) Nicolini, C.; Erokhin, V.; Paddeu, S.; Sartore, M. *Nanotechnology* **1998**, *9*, 223−227.

PM produce large "on" and "off" electrical currents. Unless such signals are kinetically resolved on micro- and millisecond time scales, they look similar, whatever the orientation or the randomness of the membrane *z*-axis distribution.[43−47] Moreover, many factors such as the pH[44] and the electrode potential[46] can affect both the intensity and/or the direction of the photogenerated currents. Also, one cannot rule out the possibility that the increased photoresponse obtained with PM films formed by the electric field-assisted technique simply results from the building of multilayers. Unless all those variables are carefully controlled, it seems to us that any conclusion as to the bR orientation in such films is premature. Nonetheless, total absence of sidedness does not prevent the generation of electric signals upon illumination of PM monolayers. Thus, it is not surprising to find that PM monolayers prepared without a special orientation procedure[3] do effectively show photoelectric signals identical to those obtained from randomly distributed patches.

Despite their *z*-dimension random distribution, monolayers built from pure and native purple patches appear, above all, as a quite stable material, once formed and equilibrated under lateral pressures higher than 10 mN/m; those films then remain stable for hours. When we compare results obtained from the various techniques in situ at the air−water interface used in the present study, it can be suggested that surface pressures of approximately 20 mN/m are ideal for the eventual use of PM films to assemble bioelectronic devices. In fact, those PM films exhibit a maximum in compactness in the *x* and *y* dimension, are the most homogeneous relative to the *z*-axis in this surface pressure range, and display a maximum in surface potential, while preserving their highly organized monolayer character. Moreover, we have also shown that bR remains photoactive in this environment, clearly displaying its typical 13-cis to all-trans photoisomerization of the protein's retinal chromophore. Given such physical stability and homogeneity, together with their biochemical, crystalline, and photoactive integrity, PM films can be viewed as a suitable material for molecular devicing.

Acknowledgment. We are indebted to the Natural Sciences and Engineering Research Council of Canada and to the Fonds FCAR (team grant to C.S. and F.B.) for financial support. M.M. also thanks the Fonds FCAR for a scholarship. C.S. is a chercheur boursier national of the Fonds de la Recherche en Santé du Québec. P.D. is a recipient of a doctoral fellowship from the Canadian Institutes of Health Research and Gimbel Eye Foundation. Ames Laboratory is operated for the U.S. Department of Energy by Iowa State University under Contract W-7405-Eng-82. The work at Ames was supported by the Director for Energy Research, Office of Basic Energy Sciences. M.M. also thanks Mm. Éric Trudel and Marc-André Laurin for technical assistance with the illustrations.

LA0356147

(43) Wang, J.-p.; Song, L.; Yoo, S.-k.; El-Sayed, M. A. *J. Phys. Chem. B* **1997**, *101*, 10599−10604.
(44) Wang, J.-P.; Yoo, S.-K.; Song, L.; El-Sayed, M. A. *J. Phys. Chem. B* **1997**, *101*, 3420−3423.
(45) Koyama, K.; Miyasaka, T.; Needleman, R.; Lanyi, J. K. *Photochem. Photobiol.* **1988**, *68*, 400−406.
(46) Saga, Y.; Watanabe, T.; Koyama, K.; Miyasaka, T. *J. Phys. Chem. B* **1999**, *103*, 234−238.
(47) Déry, M. Ph.D. Thesis Origine et signification des photocourants mesurés dans des jonctions métal-bactériorhodopsine, Université du Québec à Trois-Rivières, Trois-Rivières, Québec, 1999.